Journal of
Nanoscience and Nanotechnology
Vol. 10, 7366–7369, 2010

Formation of Catalyst Particles for Carbon Nanocoil Growth

Juanjuan Qian[1], Lujun Pan[1,*], Dawei Li[1], Naisen Yu[2], and Dongping Liu[2]

[1] *School of Physics and Optoelectronic Technology, Dalian University of Technology, Ganjingzi District, Dalian, Liaoning 116024, China*
[2] *Institute of Optoelectronic Technology, Dalian Nationalities University, Economic Development Area, Dalian, Liaoning 116600, China*

We have studied the formation process of Fe–Sn–O catalyst particles in the initial stage of carbon nanocoil synthesis by a thermal chemical vapor deposition method. A series of variance in height and morphology of catalyst particles are observed in the processes of calcination and reduction of catalyst, absorption of carbon and also the sequential growth of carbon nanocoil buds. It is found that the catalyst precursors with nanoscaled porous structures are formed on the substrate after calcination. By continuous feeding a small amount of acetylene in the reaction chamber, these precursors are gradually deoxidized and then generate lots of Fe–Sn metallic particles with different shapes, which migrate and aggregate with each other. The sizes of these particles increase continuously in the carbon absorption process. After feeding acetylene for 500 s, carbon nanocoil buds have been grown out with catalyst particles on their tips. It is noted that the catalyst particles for carbon nanocoil growth have favorite sizes of 100 to 200 nm, while the particles with other sizes tend to induce the growth of carbon nanofibers.

Keywords: Chemical Vapor Deposition, Porous Structures, Catalyst Particles, Catalyst Aggregates, Carbon Nanocoil Buds.

1. INTRODUCTION

Carbon nanocoils (CNCs) have many potential applications due to their unique helical nanostructures, excellent electromagnetic and mechanical characteristics. They are expected to be used as electromagnetic wave absorbers, microsensors, resonating elements and nanosprings etc.[1–6] These attractive applications have attracted much effort for the fabrication of CNCs, such as selecting an efficient catalyst for CNC growth and exploring their growth mechanism. In the techniques for fabrication of CNCs, selection of efficient catalysts is crucial for CNC growth, which has been studied in a lot of papers. Some metals and their alloys, such as Fe, Co, Ni, Ta, Sn can be used for catalytic synthesis of CNCs.[7–13] To date the catalyst of Fe–Sn (In)–O is considered to be highly efficient for CNC growth. Okazaki et al. have synthesized CNCs in high yield by using Fe–In–Sn–O nanoparticles prepared by a co-precipitation method.[7] Xu et al. have synthesized CNCs by using a mixed powder of iron oxide and tin oxide without addition of In.[9] Kanada et al. have succeeded in synthesizing multi-walled CNCs by using co-deposited Fe–Sn film as the catalyst.[14] We have also synthesized CNCs in high yield by using Fe and Sn containing catalysts. All these experiments suggest that Fe–Sn–O is a suitable catalyst for highly efficient growth of CNCs.

In the study of the mechanism of CNC growth, Pan et al. have determined the compositions of Fe–Sn(In)–O catalysts and suggest that Fe leads to the growth of carbon nanotubles, while In–Sn–O induces their helical growth.[15–16] Furthermore, Nishimura et al. have investigated the structural changes of a Fe–In–Sn–O catalyst film for synthesizing CNCs in chemical vapor deposition (CVD) process by a method of *in-situ* X-ray diffraction (XRD) analysis.[17] It was clearly observed from the obtained XRD spectrum that the catalyst particles were deoxided firstly, and then were changed to carbide of $Fe_3In(Sn)C$ from which CNCs were probably grown. However, these observation and analysis were performed on the whole area of the catalyst films. The behavior of a single catalyst particle has not been reported so far, which is considered to be an important and direct evidence to explain the growth mechanism of CNCs. In this paper we have studied the morphological and structural changes of discrete Fe–Sn–O catalyst particles in a thermal CVD process.

*Author to whom correspondence should be addressed.

1533-4880/2010/10/7366/004 doi:10.1166/jnn.2010.2759

2. EXPERIMENTAL DETAILS

Catalyst particles used in this study were produced by a solution method. 7.997 g $Fe_2(SO_4)_3$, 1.504 g $SnCl_2 \cdot 5H_2O$ and 6.304 g $C_6H_8O_7 \cdot H_2O$ were dissolved with 100 ml ethanol, and the solution was stirred at room temperature for an hour to make three kinds of materials mixed adequately. A droplet of the solution of 15 μl was spin-coated on a SiO_2 substrate (8 mm × 8 mm) and dried at 80 °C, then the substrate was calcined at 700 °C for 30 min in air to form the oxides of iron and tin. CNCs were synthesized at 700 °C by a thermal CVD method in the flow of Ar and acetylene with flow rate of 260 and less than 1 sccm, respectively. The deposition time was ranging from 2 to 500 s. The deposits were characterized by an atomic force microscopy (AFM), a scanning electron microscopy (SEM), an energy dispersive X-ray spectroscopy (EDX).

3. RESULTS AND DISCUSSION

Figure 1(a) shows the SEM micrograph of catalyst calcined at 700 °C in air for 30 min. It is observed that the catalyst aggregates distribute uniformly and the distance between the two catalyst clusters is approximately 5 μm. Figure 1(b) is the enlarged SEM micrograph of a typical single aggregate with a diameter of approximately 1 μm. Nanoscaled porous structures can be seen in the surface area of the catalyst aggregate, which is considered to be formed by the aggregation of nanosized oxidized particles in addition to the release of SO_3 by the thermal decomposition of $Fe_2(SO_4)_3$. This kind of structure has a large surface area that is in favor of increasing the reaction activity of the catalyst aggregate. Figure 1(c) shows the AFM topographic image and its cross section of an isolated catalyst aggregate after calcination. The catalyst aggregate has a plane size of 1 μm and a height of only 100 nm, showing a reversed-dish-like morphology. The EDX spectrum of a catalyst aggregate after calcinations is shown in Figure 2(a). The peaks corresponding to iron and tin are observed, which is originated from Fe_2O_3 and SnO_2, respectively. The molar ratio of Fe to Sn in the catalyst aggregate is calculated to be 5:2, which is similar to that in the solution.

Figures 3(a–f) show a series of SEM micrographs indicating the morphological changes of a catalyst aggregate by feeding acetylene of less than 1 sccm for 2 to 100 s. In the feeding time of 2 s, a few particles are formed and protruded out from the surface of a catalyst aggregate, around which some smaller particles are observed to be forming, as shown in Figure 3(a). It is considered that some active points exist on catalyst surface after calcination due to the inconstant compositional distribution in catalysts. The catalysts at the active points are prior to be reduced under the limited amount of acetylene and then the reduced metallic nanoparticles start to fuse with each other and are carbonized to form larger particles on the surface of the catalyst aggregate.

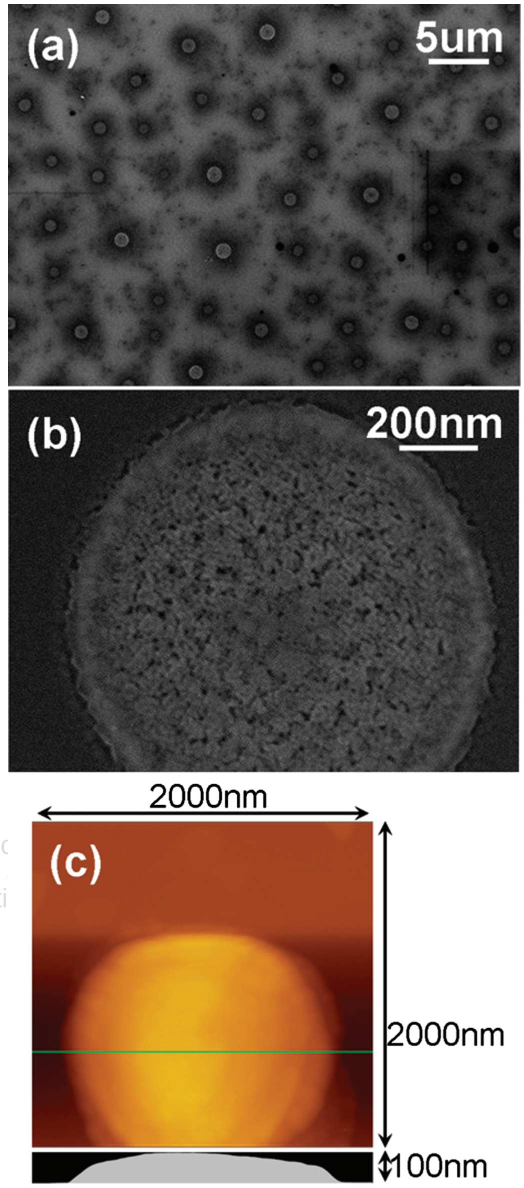

Fig. 1. (a) SEM image of catalyst aggregates after calcination at 700 °C for 30 min, (b) the enlarged SEM image of a single catalyst aggregate, and (c) AFM topographic image and its cross section of a catalyst aggregate calcined at 700 °C for 30 min.

After continuous feeding of acetylene for 5 to 10 s, nanoscaled porous structures are clearly observed in Figures 3(b and c), which is due to the self arranged migration and fusion of the reduced metallic nanoparticles. This phenomenon is kept on with the increase of feeding time to 50 and 100 s, as shown in Figures 3(d) and (e), respectively. Large particles with different kinds of shapes, most of which have a size of less than 200 nm, are formed and isolated with each other when the feeding time reaches 100 s. The EDX spectrum of catalyst after feeding acetylene for 50 s is shown in Figure 2(b). It is calculated

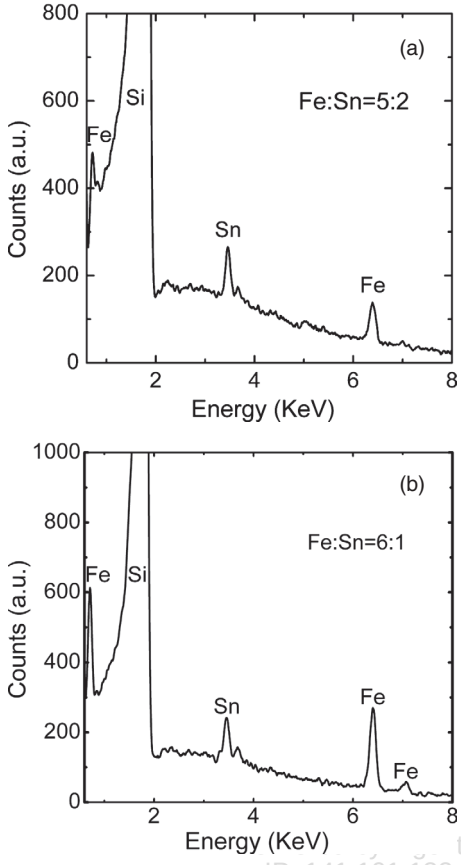

Fig. 2. EDX spectra of a catalyst aggregate (a) calcined at 700 °C for 30 min and (b) deoxidized by feeding acetylene for 50 s.

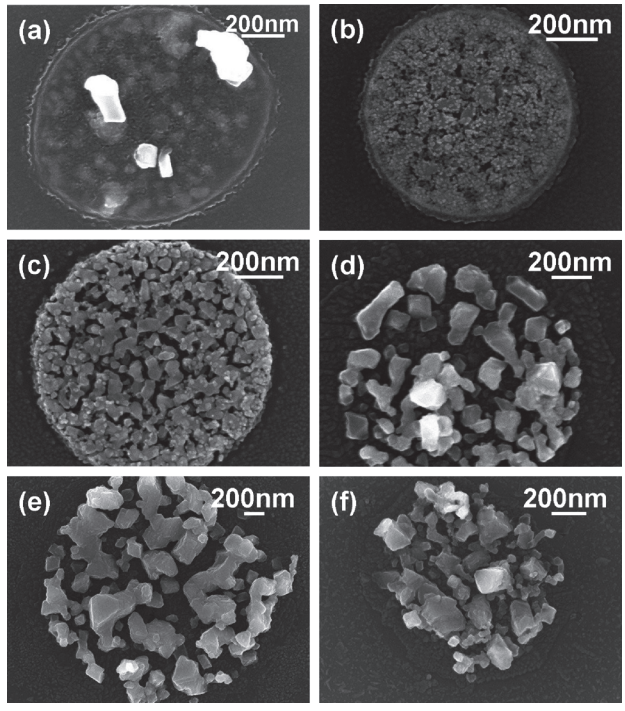

Fig. 3. SEM images of catalyst aggregate on the substrates with feeding acetylene (less than 1 sccm) at 700 °C for (a) 2 s, (b) 5 s, (c) 10 s, (d) 20 s, (e) 50 s, (f) 100 s.

that the molar ratio of Fe to Sn is 6:1, which is larger than that of the calcined catalyst in Figure 2(a), indicating that the content of Sn in the catalyst aggregate obviously decreases. This result is considered to be the evaporation of Sn from the surface of the reduced metallic nanoparticles due to the low melting point and high volatility of Sn. When the feeding time reaches 100 s the catalyst particles begin to absorb carbon atoms, which lead to the volume expansion of the catalyst particles as show in Figure 3(f).

Figure 4 shows the AFM topographic images and the corresponding cross sections of catalyst aggregates by feeding acetylene for (a) 2 s, (b) 5 s, (c) 50 s, and (d) 100 s. Consistent with the SEM images of Figure 3(a), only a few large particles with a height of approximate 100 nm protrude from the surface of the catalyst aggregate in Figure 4(a). With the proceeding of catalyst reduction by continuous feeding of acetylene for 5 to 100 s, the height of the catalyst particles gradually increases from 80 to 170 nm due to the migration and fusion of reduced catalyst particles and also the absorption of carbon.

Figure 5 shows the SEM images of samples after feeding acetylene for (a) 200 s and (b) 500 s. It is observed from Figure 5(a) that carbon materials have been precipitated from the surfaces of catalyst and some carbon fibers have been grown from the small particles on the bottom of catalyst aggregate. In Figure 5(b) some germinations of CNCs appear after feeding acetylene for 500 s. These results are also consistent with those obtained from the conventional CVD methods that the CNCs are not grown until the feeding time reaches 3 min.[18] The arrows point to the catalyst particles at the tips of CNCs buds, indicating a tip growth mechanism. It is also observed that the catalyst particles at the tips of the CNC buds have sizes of 100 to 200 nm, while the catalyst particles with sizes less than

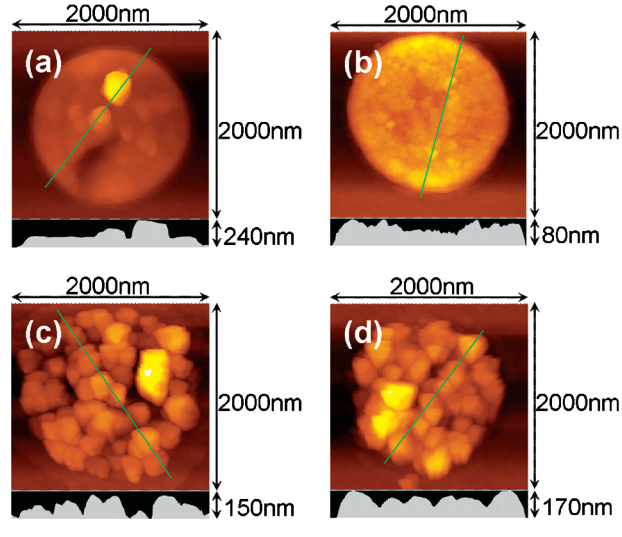

Fig. 4. AFM topographic images of a single catalyst aggregate in the cases of acetylene feeding times of (a) 2 s, (b) 5 s, (c) 50 s and (d) 100 s. The lower figures show the cross sections along the line drawn in the corresponding images.

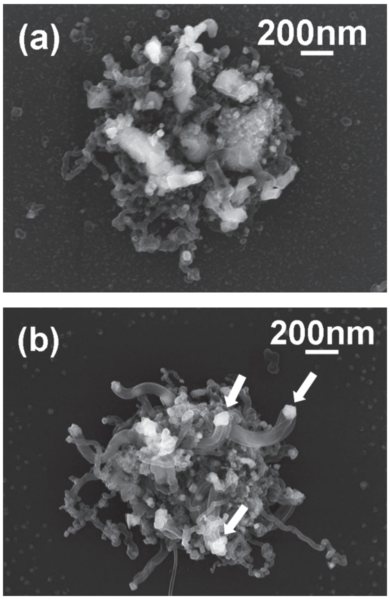

Fig. 5. SEM images of samples by feeding acetylene for (a) 200 s and (b) 500 s.

100 nm lead to the growth of carbon fibers. No fiber or CNC can be grown from the larger particles with sizes of larger than 200 nm.

4. CONCLUSIONS

The formation of catalyst particles for CNC growth has been studied. Well-distributed catalyst aggregates were obtained by the spin coating technology and Fe–Sn–O catalyst aggregates with nanoscaled porous structures were formed after calcination. With continuously feeding of acetylene, Fe–Sn–O catalysts are reduced into Fe–Sn alloy nanoparticles with a low melting point, and the reduced nanoparticles migrate and fuse with each other to form larger particles with different shapes. The volume of catalyst particles increases due to the absorption of carbon and finally leads to the growth of CNCs after the supersaturated absorption of carbon. It is found that catalyst particles with sizes of 100 to 200 nm are on the tips of CNC buds, indicating a tip growth mechanism, while particles with the sizes less than 100 nm prefer to the growth of carbon nanofibers.

References and Notes

1. S. Amelinckx, X. B. Zhang, D. Bernaerts, X. F. Zhang, V. Lvanov, and J. B. Nagy, *Science* 265, 635 (**1994**).
2. M. Zhang, Y. Nakayama, and L. Pan, *Jpn. J. Appl. Phys.* 39, 1242 (**2000**).
3. L. Pan, T. Hayashida, and Y. Nakayama, *J. Mater. Res.* 17, 145 (**2002**).
4. S. Hokushin, L. Pan, Y. Konishi, H. Tanaka, and Y. Nakayama, *Jpn. J. Appl. Phys.* 46, 565 (**2007**).
5. T. Hayashida, L. Pan, and Y. Nakayama, *Physica B* 323, 352 (**2002**).
6. L. Pan, Y. Konishi, H. Tanaka, O. Suekane, T. Nosaka, and Y. Nakayama, *Jpn. J. Appl. Phys.* 44, 1652 (**2005**).
7. N. Okazaki, S. Hosokawa, T. Goto, and Y. Nakayama, *J. Phys. Chem. B* 109, 17366 (**2005**).
8. L. Pan, M. Zhang, and Y. Nakayama, *J. Appl. Phys.* 91, 10058 (**2002**).
9. G. C. Xu, B. B. Chen, H. Shiki, T. Katsumata, H. Takikawa, T. Sakakibara, S. Itoh, and T. Ina, *Jpn. J. Appl. Phys.* 44, 1569 (**2005**).
10. Z. Y. Huang, X. Chen, J. R. Huang, M. Q. Li, and J. H. Liu, *Mater. Lett.* 60, 2073 (**2006**).
11. S. Yang, X. Chen, N. Kikuchi, and S. Motojima, *Mater. Lett.* 62, 1462 (**2008**).
12. N. J. Tang, Y. Yang, K. Lin, W. Zhong, A. Chaktong, and Y. W. Du, *J. Phys. Chem. C* 112, 10061 (**2008**).
13. S. Motojima, S. Asakura, T. Kasemura, S. Takeuchi, and H. Lwanaga, *Carbon* 34, 289 (**1996**).
14. R. Kanada, L. Pan, S. Akita, N. Okazaki, K. Hirahara, and Y. Nakayama, *Jpn. J. Appl. Phys.* 47, 1949 (**2008**).
15. L. Pan, T. Hayashida, A. Harada, and Y. Nakayama, *Physica B* 323, 350 (**2002**).
16. L. Pan, M. Zhang, and Y. Nakayama, *J. Appl. Phys.* 91, 10058 (**2002**).
17. K. Nishimura, L. Pan, and Y. Nakayama, *Jpn. J. Appl. Phys.* 43, 5665 (**2004**).
18. Y. Nakayama, L. Pan, and T. Hayashida, *Proc. IS&T's NIP18: International Conference on Digital Printing Technologies*, Academic Press, San Diego (**2002**), p. 458.

Received: 4 September 2009. Accepted: 30 October 2009.